

# The Fabrication of Biodegradable Nanofibrous Scaffold for Vascular Tissue through the Blend Electrospinning

Mustafa Aidin\*, Jamal Rahmatoglu

Department Computational chemistry, HiTech Institute of Theoretical and Computational Chemistry, India

Received: 09 April 2020

Accepted: 16 May 2020

Published: 01 June 2020

## Abstract

**Introduction:** A vascular scaffold must not only support appropriate structural integrity until neotissue can form, but also closely mimic the strength and compliance of native blood vessels. Hemocompatibility is also clearly a crucial factor to raise success of the engineered construct since the vascular scaffold comes in contact with blood. The degradation profile of the scaffold is another important criterion to consider for successful applications in tissue engineering of load-bearing structures like blood vessel tissues. A tissue-engineered vascular graft requires complete scaffold degradation with well-defined cellular organization and tissue remodeling.

**Results:** To cover all these required features, we carried out the blend electrospinning to fabricate nanofibers of poly(L-lactide acid-co-poly  $\epsilon$ -caprolactone) (PLCL), a biodegradable and compliant polymer, gelatin (Gel), a biodegradable and commercially available natural biopolymer possessing many integrin binding sites (such as RGD) for cell adhesion, and Tecophilic (TP), a hydrophilic, elastic and hemocompatible polyether-based thermoplastic aliphatic polyurethane, with a weight ratio of 60:20:20 (PGT;60/20/20) resulted in creation of a compliant, hemocompatible and biodegradable scaffold. The nanofibrous structure of the scaffold was visualized using a scanning electron microscope (SEM). The surface characterization of scaffold was carried out using ATR-FTIR spectroscopic analysis. For evaluating the potential of electrospun PGT;60/20/20 scaffold as a substrate for vascular regeneration, we cultured human aortic smooth muscle cells (SMCs) on the scaffold and studied the biocompatibility of the structure by performing the proliferation assay and cell morphology assessment.

**Conclusion:** SEM images demonstrated that electrospun PGT;60/20/20 nanofibers were successfully produced with a fiber diameter of  $459 \pm 198$  nm which revealed a significant reduction compared to fiber diameter of electrospun pure PLCL and pure TP. ATR-FTIR analysis confirms the presence of all components within the fibers. Comparing the behavior of SMCs on PGT;60/20/20 scaffolds with that on electrospun PLCL and TP scaffolds confirmed the potential use of PGT;60/20/20 nanofibers in blood vessel tissue engineering.

**Keywords:** Vascular Tissue Engineering; Electrospinning; Nanofibers; Smooth Muscle Cells

## How to cite the article:

M. Aidin, J. Rahmatoglu, *The Fabrication of Biodegradable Nanofibrous Scaffold for Vascular Tissue through the Blend Electrospinning*, Medbiotech J. 2020; 4(2): 62-69, DOI: 10.22034/MBT.2020.109581.

©2020 The Authors. This is an open access article under the CC BY license

## 1. Introduction

In this study, we utilized an electrospinning approach to fabricate biodegradable and compliant

PGT scaffolds to mimic the fibrous structural and mechanical properties of native arteries while blood compatibility was prioritized and considered

\* Corresponding Author Email: m.aidin@iitcc.org

through selecting TP, a hemocompatible polyurethane, as a main component of the scaffolds. Polymer blending is one of the most effective methods for providing amalgamated properties of several polymeric materials of the blend.

Electrospinning process is a very complex process and is associated with the interaction of several physical instability processes. According to Reneker and Chun, the stable electrospinning jet is composed of four regions: the base, the jet, the splay, and the collection. In the base region, the jet emerges from the needle to form a cone known as the Taylor cone. The shape of the base depends upon the surface tension of the liquid and the force of the electric field. If the electric field is strong enough, the jets can be ejected from surfaces that are essentially flat. Solutions of higher conductivity being more conducive are easy for jet formation. Then the electric forces accelerate and stretch the polymer jet, causing the diameter to decrease as its length increases. Solvents with high vapor pressures may begin to evaporate, causing a decrease in jet diameter and velocity. The charge repulsions cause the jet to “splay” into many small fibers of approximately equal diameter and charge per unit length [1]. Rutledge et al. have reported high-speed photography with exposure times as low as 18 ns to demonstrate that the jet that appears to splay is actually a single, rapidly whipping jet. After traveling to a short distance in high electric fields, the jet becomes unstable, begins to whip with a high frequency, and undergoes bending and stretching [2]. Rutledge et al. examined the competition between these instabilities for various applied electric fields, flow rates, and determined the dominant mode. They constructed operating diagrams that outlined the conditions at which whipping could be expected; their predictions agreed well with experimental results [2].

Blood vessels form compact closed circulatory circuits, with functions far more than conducting blood from heart to other tissues. The diverse function performed by blood vessels is facilitated by the presence of complex extracellular matrix (ECM) of blood vessels. The ECM of a blood vessel varies in its composition, thickness, and overall architecture ranging from arteries, capillaries to veins. Thus, it poses a difficult task for drawing a line of symmetry in tissue engineering approach while choosing an appropriate scaffold material for tissue engineered vascular conduits [3]. The lack of integrity in spatial and temporal level of ECM, makes it a challenging field of active investigation in tissue engineering perspectives. ECM functions include the maintenance of histological pattern of a blood vessel bearing the mechanical load imposed by moving blood. It acts as a scaffold providing major cues that direct vascular cell proliferation,

migration, attachment, and proper physiological functions. It also sequesters growth factors and plays a role in growth, remodeling and regeneration of the blood vessel both through vasculogenesis and angiogenesis. The restoration of standard vascular function and structural integrity, with neovessel formation during vascular senescence and damage forms the basis of vascular regeneration. Tissue engineered vascular regeneration aims toward the development of vascular substitutes that can regenerate in vivo and function similar to a native vessel [3].

In particular, we fabricated and characterized PLCL, TP and PGT scaffolds for engineering of the vascular tissues. Furthermore, we studied SMC behavior including attachment, proliferation, and morphology on the developed scaffolds [4-7].

## 2. Materials and Methods

### 2.1. Materials

PLCL (70:30, Mw~150 kDa) was purchased from Boehringer Ingelheim Pharma GmbH & Co. TP with a product name of SP-80A-150 was obtained from Sigma-Aldrich. Gel type A (300 Bloom) from porcine skin, 1,1,1,3,3,3hexafluoro-2-Propanol (HFP) and phosphate buffered saline (PBS) were all purchased from Sigma-Aldrich. Human aortic SMCs and smooth muscle cell medium (SMCM) were obtained from ScienCell Research Company.

### 2.2. Fabrication of scaffolds

Polymeric solutions were prepared by dissolving PLCL, Gel and TP with weight ratios of 100:0:0, 0:0:100, and 60:20:20 in HFP to obtain a total concentration of 8% (w/v), followed by 24 h stirring at room temperature. The polymeric solutions were individually loaded into a syringe and a high voltage electric field was applied to draw the fibers from the spinneret (27 G needle) onto the collector plate covered with aluminum foil. A distance of approximately 12 cm was maintained between the flat tipped spinneret and the collector plate. Solutions were fed at a constant feed rate of 1 mL/h using a syringe pump. Subsequently, the fibers were vacuum dried to remove any residual solvent and used for further experiments [8-12].

### 2.3. Characterization of nanofibrous scaffolds

The electrospun nanofibers were sputter-coated with gold (JEOL JFC-1200 Fine Coater) and visualized using a field emission scanning electron microscope (SEM; FEI-QUANTA 200F). The average diameter of the nanofibers was calculated from among 80–100 random points chosen from the SEM images, using image analysis software (Image J, National Institute of Health). The surface chemical

analysis of scaffolds was carried out using Attenuated total reflectance Fourier transform infrared (ATR-FTIR) spectroscopic analysis on Avatar 380 (Thermo Nicolet, Madison, MA) over a range of 400–4,000  $\text{cm}^{-1}$  at a resolution of 2  $\text{cm}^{-1}$ .

#### 2.4. Cell culture

SMCs were cultured at 37°C in a humidified atmosphere of 5%  $\text{CO}_2$  in a 150  $\text{cm}^2$  cell culture flask using the smooth muscle cell medium (SMCM) for 6 days and the culture medium was changed every 3 days. Electrospun fibers placed in a 24-well plate were sterilized under ultraviolet (UV) radiation for 2 h, washed twice with PBS, and subsequently immersed in SMCM overnight before cell seeding. Confluent HASMCs were trypsinized, centrifuged, counted and seeded on electrospun scaffolds and tissue culture polystyrene (TCP) as the control at a density of 10,000 cells per well [12-17].

#### 2.5. Biocompatibility assessment

The proliferation of cells on different electrospun scaffolds was monitored after 1, 4, 7, and 10 days by 3-(4,5-dimethylthiazol-2-yl)-5-(3-carboxymethoxyphenyl)-2-(4-sulfophenyl)-2H-tetrazolium (MTS) assay (CellTiter 96 Aqueous One solution; Promega). After desired time points, the cell-scaffold constructs were rinsed with PBS, and incubated with 20% MTS reagent in serum-free medium for 3h. The mixture was aliquoted into 96-well plates and read using a spectrophotometric plate reader (Fluostar Optima, BMG Lab Technologies) at 490 nm [17-21].

Morphological evaluation of SMCs on PLCL and PGT scaffolds was performed after 4 days of cell culture by SEM analysis. The cell-scaffold constructs were rinsed with PBS, fixed in 3% glutaraldehyde for 3h, rinsed with DI water, followed by dehydrating with a graded series of ethanol solution (50, 70, 90, and 100 %). Then, the samples were treated with hexamethyldisilazane (Sigma Aldrich), air-dried, and observed under SEM [22-26].

#### 2.6. Statistical Analysis

All data presented are expressed as mean $\pm$ standard deviation (SD). Statistical analysis was performed by performing one-way ANOVA followed by a Tukey's post hoc test for multiple-comparison of different samples using S-PLUS (TIBCO Software). A value of  $P < 0.05$  was considered statistically significant [27-31].

### 3. Results and Discussion

The main objective of this study was to fabricate nanofibrous scaffolds using electrospinning technique to create an optimized matrix to mimic the native vascular tissues and study SMC behavior. The SEM images of electrospun PLCL, TP and PGT scaffolds are shown in Figure 1, where randomly arranged beadless fibers with fiber diameters of  $404 \pm 95$  nm,  $881 \pm 228$  nm, and  $459 \pm 198$  nm were obtained, respectively which revealed a significant reduction in fiber diameter of PGT scaffolds by incorporation of gelatin within nanofibers ( $P < 0.05$ ) [30-35].

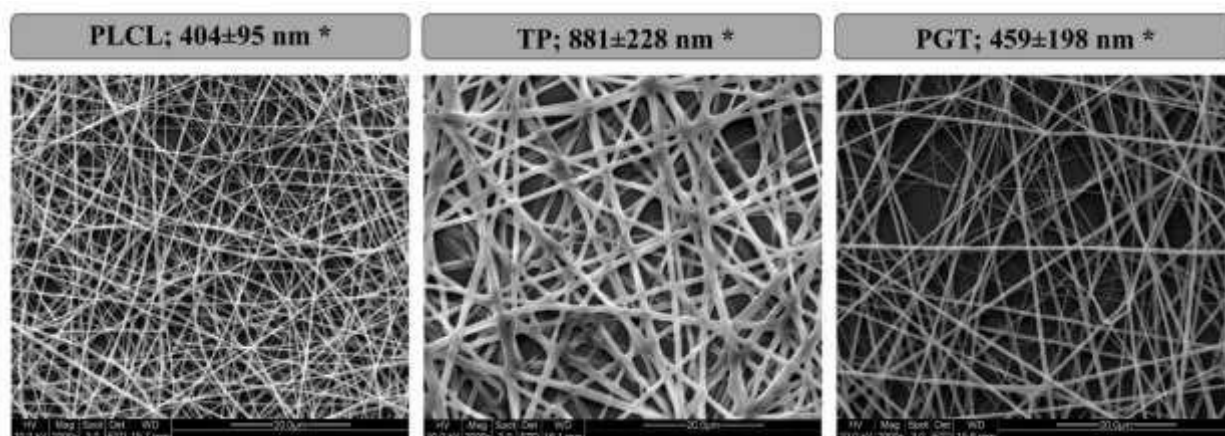


**Figure 1.** SEM micrographs of electrospun scaffolds indicates significant differences compared to PGT

Incorporation of gelatin within the PGT fibers was confirmed by FTIR analysis. ATR-FTIR spectra of pure PLCL, TP, and Gel as well as their blend together are shown in Figure 2 [36-41].

These spectra reveal the presence of characteristic bands for PLCL in the PGT scaffold. These includes 1756  $\text{cm}^{-1}$ , 1735  $\text{cm}^{-1}$  corresponding to C–O

stretching in poly(L-lactide) and poly( $\epsilon$ -caprolactone), respectively, 1380  $\text{cm}^{-1}$  (O–H bending) and 1056  $\text{cm}^{-1}$  (C–O stretching). The presence of common indicative bands of gelatin in PGT scaffold was revealed at 1650  $\text{cm}^{-1}$  and 1540  $\text{cm}^{-1}$  which belong to the amide I and amide II peaks corresponding to the stretching vibrations of C–O

bond in the backbone of protein and coupling of N-H in plane bending and C-N stretching in the gelatin, respectively [6]. The characteristic TP-based stretching modes at 1703  $\text{cm}^{-1}$  assigned to the urethane C=O stretching, 1530  $\text{cm}^{-1}$  and 1310

$\text{cm}^{-1}$  responsible for C-N stretching and 1110  $\text{cm}^{-1}$  and 1080  $\text{cm}^{-1}$  attributed to stretching vibration of C-O-C bond in aliphatic ether of soft and hard segments of TP are also visible for PGT scaffold [42-47].

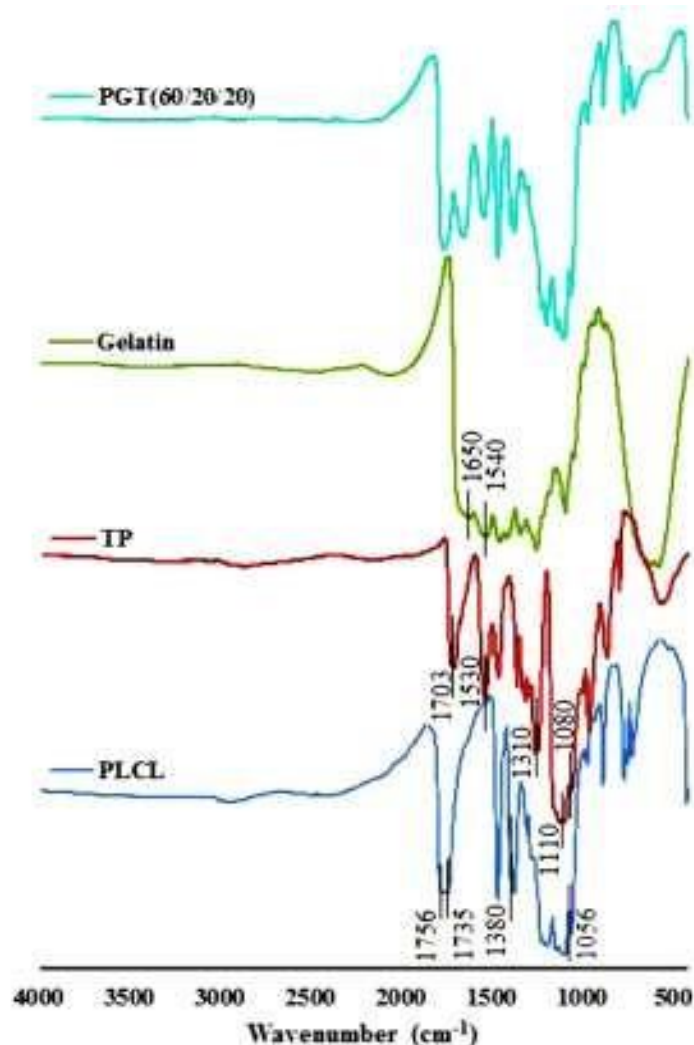


**Figure 2.** ATR-FTIR spectra of electrospun scaffolds

As a fibrous scaffold physically mimics the ECM structure of the native tissue, it provides a favorable matrix for the cellular adhesion and proliferation. The vascular scaffold should possess excellent biocompatibility to ensure that the vascular cells preserve their long-term viability and continue to grow during the reconstruction of the engineered tissue. The utility of the electrospun scaffolds for developing appropriate grafts for clinical transplantation was evaluated by MTS assays, which estimates the effect of scaffolds on the viability, growth, and metabolic behavior of SMCs (Figure 3). [41, 48-52].

As shown in Figure 3, cells continued to proliferate over time, confirming the ability of scaffolds to support cell growth, and demonstrating their noncytotoxic behavior. Upon increasing the culture time, the statistical differences in cell proliferation between the samples appeared, such that the cell number on PGT scaffolds was significantly greater than that on the electrospun PLCL and TP scaffolds but also lower compared to the cell growth on TCP on days 7 and 10 ( $p < 0.05$ ). The incorporation of gelatin created numerous cell binding ligands such as RGD motif on the surface of PGT scaffolds making them more favorable for cell growth and proliferation.



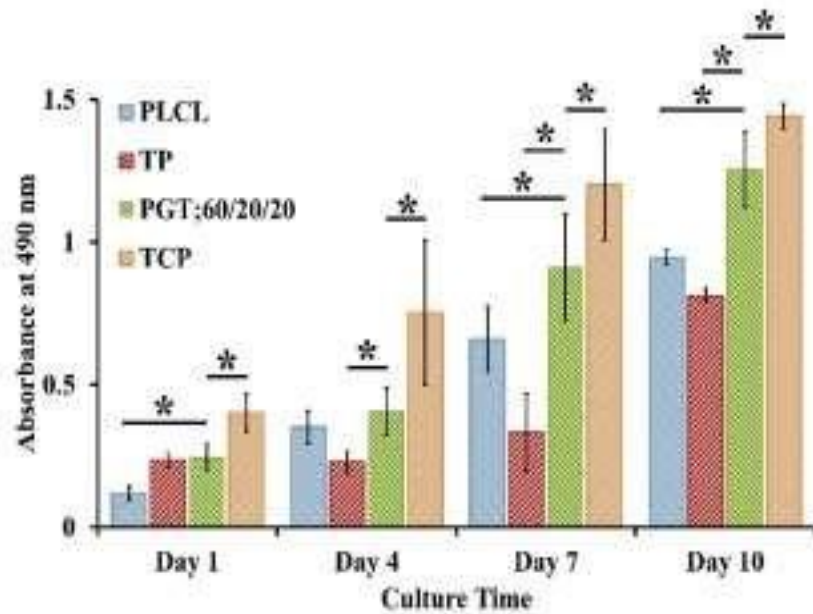


**Figure 3.** Proliferation of SMCs on electrospun PLCL, TP and PGT scaffolds; \* indicates significant differences from electrospun PGT scaffold

SEM images depicting cell adhesion, spreading, and morphology are presented in Figure 4. SMCs were found to adhere successfully to the surface of the scaffolds and TCP. As shown in Figure 4, within 4 days of cell culture, a relatively spindle shape was observed for SMCs on electrospun PLCL and PGT scaffolds confirming the capability of the scaffolds

to support SMC contractility. A successful tissue-engineered scaffold should not only facilitate cell attachment and proliferation but should also allow cells to preserve their specific phenotype. Therefore, this study approves the feasibility of electrospun PGT scaffold for development of a functional vascular graft.

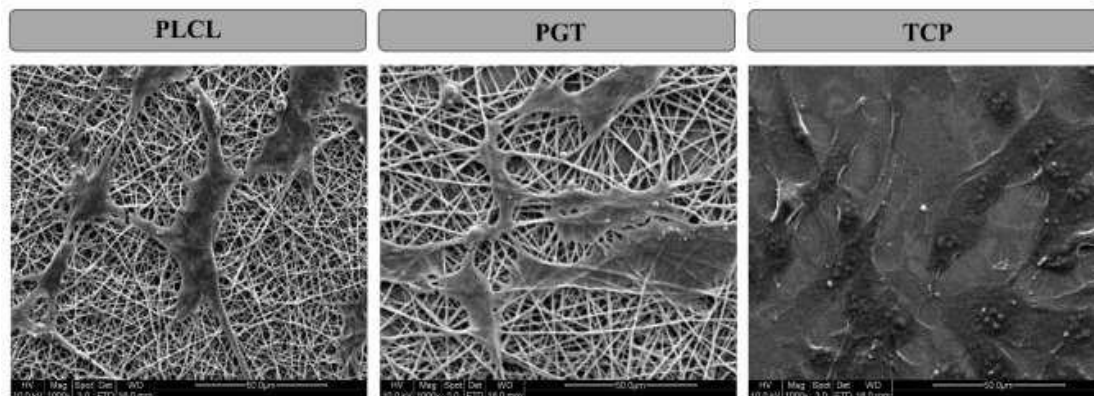


**Figure 4.** SEM images showing SMC-scaffold interactions on day 4

#### 4. Conclusion

In this study, a feasible scaffold electrospun from PLCL, Gel and TP with a weight ratio of 60:20:20 was designed to span multiple requirements of a tissue-engineered vascular graft. Our findings indicated that PGT fibrous membranes with respectable mechanical and structural properties and ability to control the behavior of SMCs can be used as a potentially suitable Scaffold for vascular tissue regeneration applications.

#### Acknowledgements

I appreciate all supports from the department of biology and Payam Noor University, Tehran, Iran.

#### Ethical Issues

This research didn't need any ethical permission from authorized department.

## References

1. Xu CY, Inai R, Kotaki M, Ramakrishna S. 2004. Aligned biodegradable nanofibrous structure: a potential scaffold for blood vessel engineering. *Biomaterials* 25(5): 877-886.
2. Chong EJ, Phan TT, Lim IJ, Zhang YZ, Bay BH, Ramakrishna S, et al. 2007. Evaluation of electrospun PCL/gelatin nanofibrous scaffold for wound healing and layered dermal reconstitution. *Acta Biomaterialia* 3(3): 321-330.
3. Swartz DD, Andreadis ST. 2013. Animal models for vascular tissue-engineering. *Current Opinion in Biotechnology* 24(5): 916-925.
4. Omid Zabihi SMM, Fatemeh Ravari, Aminreza Khodabandeh, Amin Hooshafza, Karim Zare, Mehrab Shahzadeh. 2011. The effect of zinc oxide nanoparticles on thermo-physical properties of diglycidyl ether of bisphenol A/2, 2'-Diamino-1, 1'-binaphthalene nanocomposites. *Thermochimica acta* 521(1-2): 49-58.
5. Seyed Mojtaba Mostafavi AR, Mina Adibi, Farshid Pashae, Masoumeh Piryaee. 2011. Modification of Glassy Carbon Electrode by a Simple, Inexpensive and Fast Method Using an Ionic Liquid Based on Imidazolium as Working Electrode in Electrochemical Determination of Some Biological Compounds. *Asian Journal of Chemistry* 23(12).
6. Seyed Mojtaba Mostafavi AR, Mina Adibi, Farshid Pashae, Masoumeh Piryaee. 2011. Electrochemical Investigation of Thiophene on Glassy Carbon Electrode and Quantitative Determination of it in Simulated Oil Solution by Differential Pulse Voltammetry and Amperometry Techniques. *Asian Journal of Chemistry* 23(12): 5356-5360.
7. MOSTAFAVI SM, ROUHOLLAHI A, ADIBI M, PASHAEE F, PIRYAEI M. 2011. Modification of Glassy Carbon Electrode by a Simple, Inexpensive and Fast Method Using an Ionic Liquid Based on Imidazolium as Working Electrode in Electrochemical Determination of Some Biological Compounds. *Asian Journal of Chemistry* 23(12).
8. S. MOJTABA MOSTAFAVI AR, MINA ADIBI, FARSHID PASHAEE, PIRYAEI M. 2011. Electrochemical Investigation of Thiophene on Glassy Carbon Electrode and Quantitative Determination of it in Simulated Oil Solution by Differential Pulse Voltammetry and Amperometry Techniques. *Asian Journal of Chemistry* 23(12): 5356-5360.
9. Omid Zabihi AK, Seyed Mojtaba Mostafavi. 2012. Preparation, optimization and thermal characterization of a novel conductive thermoset nanocomposite containing polythiophene nanoparticles using dynamic thermal analysis. *Polymer degradation and stability* 97(1): 3-13.
10. Mojtaba Shamsipur AAMB, Mohammad Teymouri, Tahereh Poursaberi, Seyed Mojtaba Mostafavi, Parviz Soleimani, Fereshteh Chitsazian, Shahram Abolhassan Tash. 2012. Biotransformation of methyl tert-butyl ether by human cytochrome P450 2A6. *Biodegradation* 23(2): 311-318.
11. Seyed Mojtaba Mostafavi AR, Ali Akbar Miranbeigi. Handbook of Mineral Analysis: Mani Publication, Ltd, Isfahan, Iran; 2012.
12. Seyed Mojtaba Mostafavi MP, Ahmad Rouhollahi, Ali Mohajeri. 2014. Separation and Quantification of Hydrocarbons of LPG Using Novel MWCNT-Silica Gel Nanocomposite as Packed Column Adsorbent of Gas Chromatography. *Journal of NanoAnalysis* 1(01): 01.
13. Seyed Mojtaba Mostafavi MP, Ahmad Rouhollahi, Ali Mohajeri. 2014. Separation of Aromatic and Alcoholic Mixtures using Novel MWCNT-Silica Gel Nanocomposite as an Adsorbent in Gas Chromatography. *Journal of NanoAnalysis* 1(01): 11.
14. Mostafavi SM. 2015. 3D Graphene Biocatalysts for Development of Enzymatic Biofuel Cells: A Short Review. *Journal of Nanoanalysis* 2(2): 57-62.
15. Sepideh Parvanian SMM, Meysam Aghashiri. 2016. Multifunctional Nanoparticle Developments in Cancer Diagnosis and Treatment. *Sensing and Bio-Sensing Research* 1(2): 22.
16. Mostafavi SM, editor Enhancement of mechanical performance of polymer nanocomposites using ZnO nanoparticles. 5th International Conference on Composites: Characterization, Fabrication and Application (CCFA-5); 2016: Iran University of Science and Technology.
17. Asghar Pasban SMM, Hanieh Malekzadeh, Benyamin Mohammad Nazari. 2017. Quantitative Determination of LPG Hydrocarbons by Modified Packed Column Adsorbent of Gas Chromatography Via Full Factorial Design. *Journal of Nanoanalysis* 4(1): 31-40.
18. Somayyeh Heidari MI, Seyed Mojtaba Mostafavi. 2017. A Validated and Rapid HPLC Method for Quantification of Human Serum Albumin in Interferon beta-1a Biopharmaceutical Formulation. *MedBioTech Journal* 1(01): 29.
19. Seyed Mojtaba Mostafavi KB, Masoud Amanlou. 2017. A new attempt to introduce efficient inhibitors for Caspase-9 according to structure-based Pharmacophore Screening strategy and Molecular Dynamics Simulations. *Medbiotech Journal* 01(01): 1-8. en.
20. Masoud Amanlou SMM. 2017. In silico screening to aim computational efficient inhibitors of caspase-9 by ligand-based pharmacophore modeling. *Medbiotech Journal* 01(01): 34-41. en.
21. Mostafavi SM, Pasban AA, Piryaee M, Sadeghpour S, Masoumi M, Rouhollahi A, et al. 2017. Acidity removal of Iranian heavy crude oils by nanofluid demulsifier: An experimental investigation. *Journal of Nanoanalysis*: 10-17.

22. Heidari S, Imani M, Mostafavi SM. 2017. A Validated and Rapid HPLC Method for Quantification of Human Serum Albumin in Interferon beta-1a Biopharmaceutical Formulation. *Medbiotech Journal* 1(01): 29-33.
23. Seyed Mojtaba Mostafavi AAP, Masoumeh Piryaeei, Saeed Sadeghpour, Majid Masoumi, Ahmad Rouhollahi, Ali Akbar Miran Beigi. 2017. Acidity removal of Iranian heavy crude oils by nanofluid demulsifier: An experimental investigation. *Journal of Nanoanalysis*: 10-17.
24. Aida Badamchi Shabestari BAA, Maryam Shekarchi, Seyed Mojtaba Mostafavi. 2018. Development of Environmental Analysis for Determination of Total Mercury in Fish Oil Pearls by Microwave Closed Vessels Digestion Coupled with ICP-OES. *Ekoloji* 27(106): 1935.
25. Mahya Bayat SMM. 2018. Investigation of Interleukin 2 as Signaling Molecule in Human Serum Albumin. *The Pharmaceutical and Chemical Journal* 5(02): 183-189.
26. Shabestari AB, Mostafavi SM, Malekzadeh H. 2018. Force Degradation Comparative Study on Biosimilar Adalimumab and Humira. *Revista Latinoamericana de Hipertension* 13(6): 496-509.
27. Samira Eissazadeh SMM, Masoumeh Piryaeei, Mohammad Sadegh Taskhiri. 2019. Application Of Polyaniline Nanostructure Based Biosensor For Glucose And Cholesterol Detection. *Research Journal of Pharmaceutical, Biological and Chemical Sciences* 10(1): 150.
28. Samira Eissazadeh MP, Mohammad Sadegh Taskhiri, Mostafavi SM. 2019. Improvement of Sensitivity of Antigen-Antibody Detection of Semen Through Gold Nanoparticle. *Research Journal of Pharmaceutical, Biological and Chemical Sciences* 10(1): 144.
29. Samira Eissazadeh MP, Seyed Mojtaba Mostafavi. 2019. Measurement of Some Amino Acid Using Biosensors Based on Silicon-Based Carbon Nanotubes. *Journal of Computational and Theoretical Nanoscience* 16: 1.
30. Aida Badamchi Shabestari SMM, Hanieh Malekzadeh. 2019. Force Degradation Comparative Study on Biosimilar Adalimumab and Humira. *Revista Latinoamericana de Hipertension* 13(06): 496-509.
31. Seyed Mojtaba Mostafavi HM, Mohammad Sadegh Taskhiri. 2019. In Silico Prediction of Gas Chromatographic Retention Time of Some Organic Compounds on the Modified Carbon Nanotube Capillary Column. *Journal of Computational and Theoretical Nanoscience* 16(151): 156.
32. Seyed Mojtaba Mostafavi FP, Ahmad Rouhollahi, Mina Adibi, editor Electrochemical Study and Determination of Thiophene by Cobalt Oxide Nanoparticle Modified Glassy Carbon Electrode. 6th Aegean Analytical Chemistry Days (AACD), Denizli, Turkey; 2008.
33. Seyed Mojtaba Mostafavi SE, Masoumeh Piryaeei. 2019. Comparison of Polymer and Ceramic Membrane in the Separation of Proteins in Aqueous Solution Through Liquid Chromatography. *Journal of Computational and Theoretical Nanoscience* 16(1): 157-164.
34. Saeed Jafari SAM. 2019. Investigation of nitrogen contamination of important subterranean water in the plain. *Medbiotech Journal* 03(01): 10-12. en.
35. Z. Man AGE, Seyed Mojtaba Mostafavi, A. Surendar. 2019. Fuel oil characteristics and applications: economic and technological aspects. *Petroleum Science and Technology* 37(09): 1041-1044.
36. Seyed Mojtaba Mostafavi HM, Mohammad Sadegh Taskhiri. 2019. In Silico Prediction of Gas Chromatographic Retention Time of Some Organic Compounds on the Modified Carbon Nanotube Capillary Column. *Journal of Computational and Theoretical Nanoscience* 16(01): 151-156.
37. Eissazadeh S, Piryaeei M, Taskhiri MS, Mostafavi SM. 2019. Improvement of Sensitivity of Antigen-Antibody Detection of Semen Through Gold Nanoparticle. *RESEARCH JOURNAL OF PHARMACEUTICAL BIOLOGICAL AND CHEMICAL SCIENCES* 10(1): 144-149.
38. Eissazadeh S, Piryaeei M, Mostafavi SM. 2019. Measurement of some amino acid using biosensors based on silicon-based carbon nanotubes. *Journal of Computational and Theoretical Nanoscience* 16(1): 165-167.
39. Seyed Mojtaba Mostafavi AE. 2019. Mercury determination in work place air and human biological samples based on dispersive liquid-liquid micro-extraction coupled with cold vapor atomic absorption spectrometry. *Analytical Methods in Environmental Chemistry Journal* 2(04): 49-58.
40. Eissazadeh S, Mostafavi SM, Piryaeei M, Taskhiri MS. 2019. Application Of Polyaniline Nanostructure Based Biosensor For Glucose And Cholesterol Detection. *RESEARCH JOURNAL OF PHARMACEUTICAL BIOLOGICAL AND CHEMICAL SCIENCES* 10(1): 150-157.
41. Nezhad AY, SH AMF, Piryaeei M, Mostafavi SM. 2019. Investigation of Shigella lipopolysaccharides effects on immunity stimulation of host cells. *International Transaction Journal of Engineering, Management, Applied Sciences and Technologies* 10: 465.
42. Mehdi Kargarfard RR, Ayeh Rizvandi, Mehdi Dahghani, Parinaz Poursafa. 2009. Hemodynamic physiological response to acute exposure to air pollution in young adults according to the fitness level. *ARYA Atherosclerosis* 5(3).
43. Rizvandi A, Taghipour Gharbi M, Esmaeili M, Ashraf Ganjooee F. 2019. The Evaluation of Performance Indicators of Coaches in Football

- Development. *Journal of Humanities Insights* 03(04): 248-254.
44. Aye Rizvandi MTG, Mohammadreza Esmaeili, Farideh Ashraf Ganjooee. 2019. The Evaluation of Performance Indicators of Coaches in Football Development. *Journal of Humanities Insights* 3(4).
45. Aye Rizvandi FT, Zaheh Sadegh Zadeh. 2019. Sport consumer behaviour model: Motivators and constraints. *Universidad de Alicante Área de Educación Física y Deporte* 14.
46. Aye Rizvandi FT. 2019. Entrepreneurial marketing effects on sport club manager performance (Conceptual Model). *Universidad de Alicante Área de Educación Física y Deporte* 14.
47. Aye Rizvandi MF, Maryam Asadollahi Supply Chain Management for Sporting Goods Retailing: Mikima Book Publication; 2020.
48. Narmin Najafzadeh MMS, Syed Shuja Sultan, Adel Spotin, Alireza Zamani, Roozbeh Taslimian, Amir Yaghoubinezhad, Parviz Parvizi. 2014. The existence of only one haplotype of Leishmania major in the main and potential reservoir hosts of zoonotic cutaneous leishmaniasis using different molecular markers in a focal area in Iran. *Revista da Sociedade Brasileira de Medicina Tropical* 47(5).
49. Adel Spotin SR, Parviz Parvizi, Parnazsadat Ghaemmaghami, Ali Haghghi, Aref Amirkhani, Ali Bordbar, Amir Yaghoubinezhad. 2014. Different Phenotypic Aspects with No Genotypic Heterogeneity in Leishmania Major Isolates of Suspected Patients in Northern Khuzestan Province. *Iranian Journal of Public Health* 43(2).
50. Neda Samei PP, Adel Spotin, Mohammad Reza Khatami Nezhad, Narmin Najafzadeh, Amir Yaghoubinezhad. 2014. Identifying of Causative Agents of Cutaneous Leishmaniasis by Amplifying Cyt B Gene in Indigenous Foci of Iran. *Iranian Journal of Public Health* 43(2).
51. Neda Samei PP, Mohammadreza Khatami Nezhad, Amir Yaghoubinezhad, Narmin Najafzadeh, Adel Spotin. Finding various molecular haplotypes of Leishmania major in human using three HSp70, ITS-rDNA and Cyt b genes. 1st and 13th Iranian Genetics Congress; Tehran 2014.
52. Somayyeh Heidary AYN, Atefeh Mehrabi Far. 2018. Colonization and Investigation of Vibrio Cholera Recombination Protein in E-Coli. *International Journal of Engineering & Technology* 7(4.7).